

X-611-62-128

38 p.

1065-88722

VANGUARD III

MAGNETIC FIELD OBSERVATIONS*

FACILITY FORM 602

1065-88722
(ACCESSION NUMBER)

(THRU)

(PAGES)

TMX-57482
(NASA CR OR TMX OR AD NUMBER)

(CODE)

(CATEGORY)

BY

J. C. CAIN

I. R. SHAPIRO

J. D. STOLARIK

J. P. HEPPNER

AUGUST 21, 1962



GODDARD SPACE FLIGHT CENTER
GREENBELT, MD.

*TO BE SUBMITTED FOR PUBLICATION IN
THE JOURNAL OF GEOPHYSICAL RESEARCH

TM-X 57482

1165-88722
~~X 63 14474~~
Code 2a

Vanguard III Magnetic Field Observations

Joseph C. Cain, I. R. Shapiro, J. D. Stolarik, J. P. Heppner


NASA Goddard Space Flight Center

Greenbelt, Maryland

Abstract:

14474

An analysis was made of the scalar proton magnetometer observations taken September -- December, 1959, by the Vanguard III satellite (1959 Eta). The measurements were taken near receiving stations at geographic latitudes less than 33.5° and within the altitude limits 510 to 3753 Km. Average daily storm-time (Dst) changes of the field correlate positively with those from surface observatories showing that their sources are definitely above 510 Km and very likely above 2400 Km. It was found possible to fit the observations to an RMS error of 21γ or 0.1% using a set of 63 harmonic coefficients with a potential function of only internal origin. It was not possible to obtain information on diurnal variations due to the slow change of the orbital plane in local time.



1. Introduction

Virtually all of the present information on the time fluctuations of the geomagnetic field accumulated over the past century has been based on precise measurements taken at a relatively few magnetic observatories spaced irregularly over the earth's surface. Because these measurements were limited to the surface of the earth it has never been possible to set up unique models of the sources of electric current responsible for the fluctuations. The planning of the Vanguard III magnetic experiment by Heppner, Stolarik, and Meredith, [1958b] was based on the availability of the proton magnetometer as an instrument that could accurately sample the total scalar field above the ionosphere. The main objective of this experiment was to determine whether the major source of the currents responsible for a magnetic storm lay within or above the ionosphere. If these currents were ionospheric, they would oppositely affect the horizontal component of field above the ionosphere to that below. Since only the total scalar field could be measured, a simple interpretation could be expected only in equatorial regions where the magnetic dip is small. It was also thought that some information might be obtained on the equatorial electrojet which had been located at altitudes near 100 Km by sounding rockets [Singer, Maple, and Bowen, 1951; Cahill, 1959a, b]. The measurements were also intended to check the accuracy of predicting magnetic field intensities at altitude from analyses of surface magnetic field charts.

One of the primary concerns for the success of this experiment lay in the difficulty of distinguishing spatial from temporal fluctuations

of the field. The satellite observations were not unlike those of a magnetic survey except that in this experiment it was not only necessary to map the field, but also to determine temporal fluctuations in the data. This type of study has never been attempted using conventional ground survey data since the amplitude of the spatial irregularities is normally larger than that of the time changes.

2. Satellite and Instrumentation

The Satellite

The Vanguard III satellite was launched September 18, 1959 into an orbit with an inclination of 33.5° and an initial height range from 510 to 3753 Km above the earth's surface. In addition to the magnetic field experiment the satellite contained experiments for measurements of X-rays (experiment supervised by H. Friedman of the Naval Research Laboratory) and micrometeorites [Alexander, McCracken, and LaGow, 1961]. Data were transmitted until the battery capacity was exhausted on December 11, 1959 -- a total life of 85 days. Perigee remained on the night side throughout this interval although it oscillated twice past all latitudes up to the 33.5° limit. Although non-transmitting, this satellite is still being observed optically and is expected to orbit on the order of 150 years [Zadunaisky and Miller, 1961] .

The Instrumentation

The magnetometer used was a proton precession instrument capable of making precise measurements of the total scalar magnetic field. The instrument consisted of a sensing head, a high-gain, wide-bandpass

amplifier, an 80-milliwatt, 108.03 mc/s telemetry transmitter, and a command receiver. One precession signal of about two seconds duration was produced per ground command. The command signal, via a tuned receiver in the satellite, activated a multivibrator programming circuit in the magnetometer which then: (1) turned on the 108.03 mc/s transmitter and the magnetometer amplifier; (2) connected the sensing head coil to a 12-volt battery pack for about 2 seconds, causing phase coherence of the protons in the sample by the resulting polarizing field; (3) switched the coil to the amplifier following polarization; and (4) after about 4 seconds, switched off the 108.03 mc/s transmitter and magnetometer amplifier. The 108.03 mc/s carrier frequency was amplitude-modulated by the magnetometer signal.

3. Data

Distribution of Observations

The limitation of chemical batteries and real-time data transmission provided the possibility of approximately 4000 observations within range of the receiving stations. To allow sufficient time to observe during intervals of different magnetic activity, approximately 50 interrogations per day were planned. These data were taken near the geographic meridians of the minitrack stations to provide sufficiently dense observations to simplify the problem of analyzing time fluctuations. The total number of observations suitable for analysis was 2797 with a distribution in area as shown in Figure 1. A listing of these observations including a detailed discussion of the data reduction is

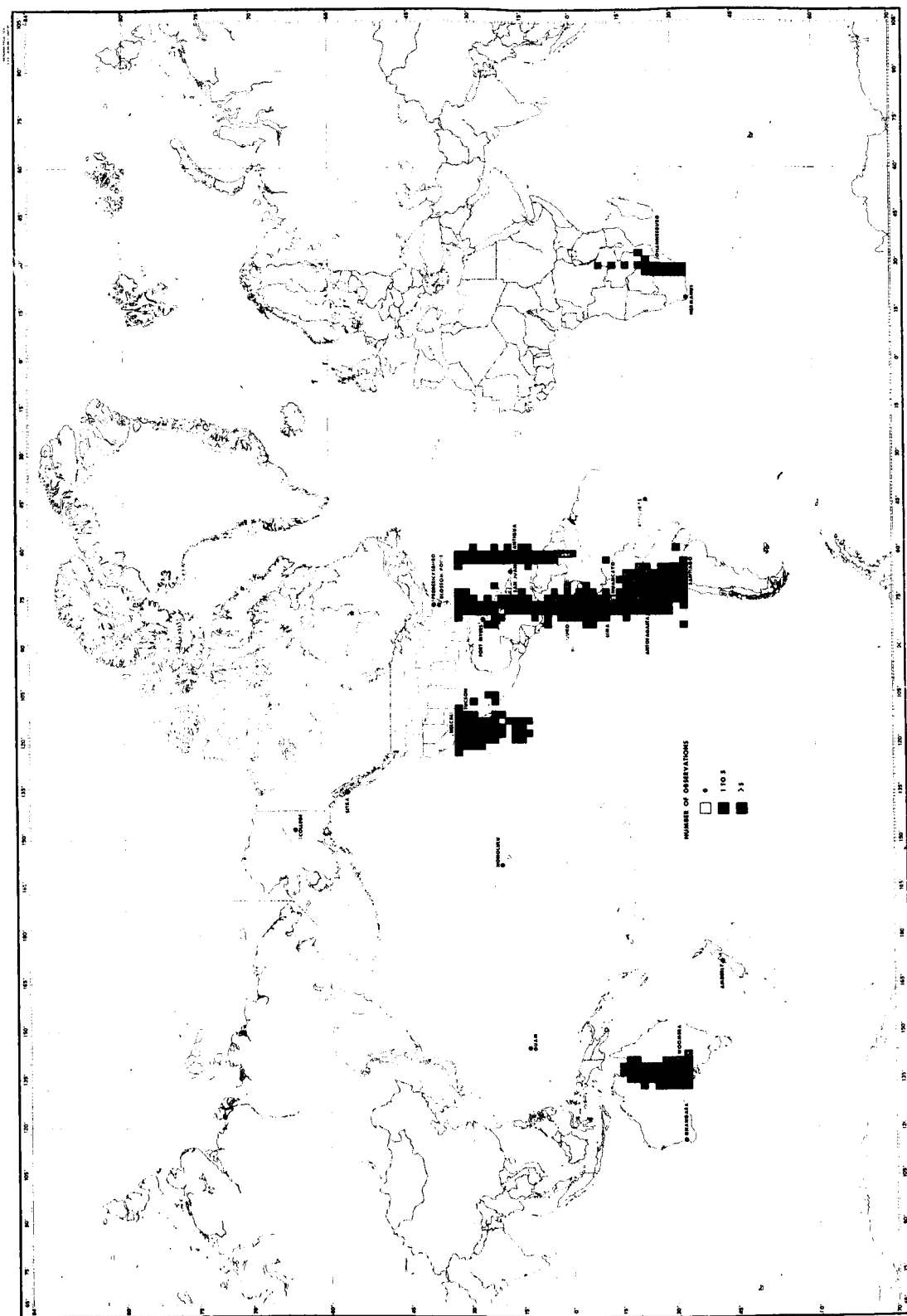


Figure 1-Distribution of magnetic data from the Vanguard III satellite. The observations are summarized in blocks of longitude and latitude 2° on a side. The cross hatched blocks contain between one and five observations whereas the black ones contain more than five. Total observations = 2797.

given by Cain, Shapiro, Stolarik and Heppner, [1962]. The data receiving stations indicated on this figure are Woomera (Australia), "Nelcal" (Chula Vista, California), Blossom Point (Maryland), Fort Myers (Florida), Antigua (British West Indies), Quito (Ecuador), Lima (Peru), Antofagasta (Chile), Santiago (Chile), and Johannesburg (Union of South Africa). The other stations indicated are the locations of standard magnetic observatories. Observation of the vector field in the vicinity of the receiving stations was also made using a vector proton installation [Shapiro, Stolarik and Heppner, 1960].

Reduction to a Reference Field

The major problem of interpreting geomagnetic measurements from a moving vehicle is that of determining a reference field. Ideally, the contribution of the earth's main field should first be subtracted vectorially from the satellite measurements. The remainder would then reflect only contributions from sources above the earth's surface and currents induced in the conducting earth by time variations of these sources. In theory, the main field could be computed at the earth's surface by an analysis of magnetic charts or survey observations and then extrapolated above the surface by such common techniques as spherical harmonic expansions. Unfortunately, the density of recent magnetic survey observations at the earth's surface is far too sparse to allow a sufficiently accurate extrapolation. Preliminary evaluations of the data were made using both the Finch and Leaton [1957] and the Jensen and Whitaker [1960] sets of spherical harmonic coefficients.

The algebraic difference $\Delta F = F(\text{measured}) - F(\text{computed})$ between the total intensities of these fields and the measured scalar intensities was up to two percent of the scalar field [Heppner, Skillman, and Cain, 1961]. The fact that these differences varied systematically with the area of measurement and with altitude strongly suggested that a more accurate reference could be obtained. An attempt at obtaining such a reference from some 75,000 magnetic survey observations was made by Jensen and Cain [1962]. This computation will be discussed in more detail elsewhere but it is pertinent here to mention that the improvement over past analyses was not striking, mainly due to the very poor distribution of available magnetic survey data. The Vanguard data themselves were included in this computation but did not significantly alter the field since they comprised only 4% of the total observations used.

In order to provide a working reference for studying the Vanguard III magnetic observations, it was found more expedient to generate a field based only on those data. The procedure used was identical to that used by Jensen and Cain [1962] in generating the epoch 1960 field except that secular changes were ignored. This elimination of the secular change was possible due to the short interval over which the data were accrued. A survey of the secular change over the regions for which data were taken indicates that the mean error resulting from this omission is of the order of a few hundredths of a percent. The three dimensional curve fitting involved making iterative linear corrections to an approximate spherical harmonic potential function in order to decrease the RMS residual of such quantities as

$$F^2 - B^2 = \Delta F^2 \quad (1)$$

$$F - B = \Delta F \quad (2)$$

$$\text{and} \quad (F - B)/F = \Delta F/F \quad (3)$$

where F is the observed scalar field and B the field computed from a spherical harmonic expansion. Since the field strength varies as a factor of about three from perigee to apogee, and less than two from the weakest to strongest area at a given altitude, such different weighting criteria mainly affect the distribution of errors with altitude. That is, minimizing ΔF^2 automatically produces a somewhat better fit to the data at low altitude due to the greater field intensity. The distribution of data with altitude is given on the left side of Figure 2. As expected from telemetry considerations, there is a preponderance of data near perigee with a slow decrease to apogee. The middle and right hand graphs show plots of the average residuals $\Delta F/F$ and ΔF respectively as a function of altitude for two separate sets of harmonic coefficients fitted to the data. The middle graph was derived using a set of 63 harmonic coefficients (g_n^m and h_n^m with n and m up to 7) obtained by minimizing the relative error $\Delta F/F$. The right hand graph was computed using a different set of 63 coefficients derived by minimizing the quantity ΔF^2 defined in Equation (1) (note that the residual plotted is ΔF and not ΔF^2). On both of these plots the error bars represent the standard error of the average. Other weightings of the data were tried in attempts to produce a reference field which had no systematic change

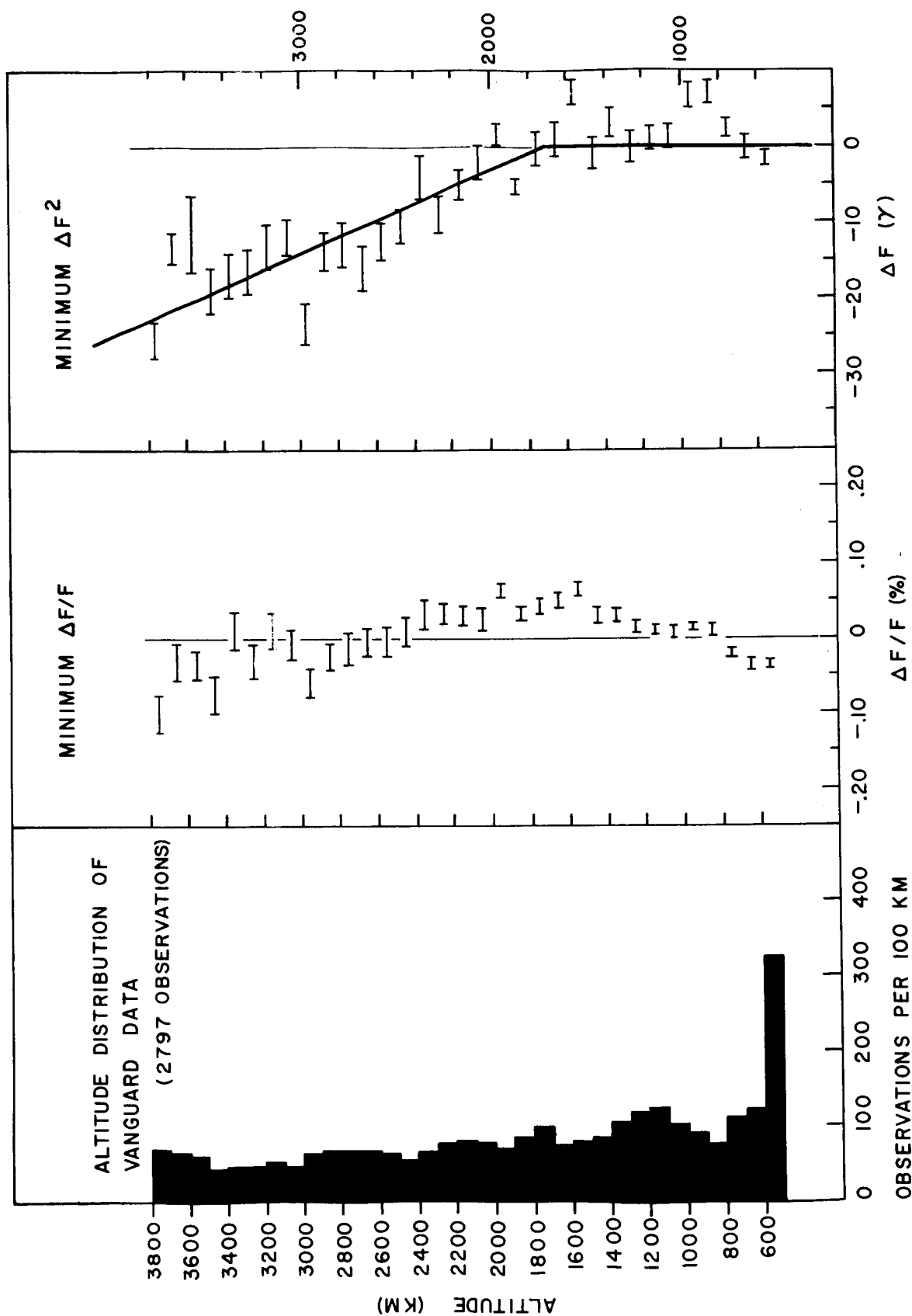


Figure 2—Average residuals of magnetometer data with altitude from two reference fields; and altitude distribution of data. The average altitude residuals are plotted as error bars indicating the standard errors of the mean. The middle graph gives residuals from a set of 63 (n, m, up to 7) spherical harmonic coefficients fitted to the Vanguard data minimizing the relative error $\Delta F/F$. The right hand graph gives the average residuals where ΔF^2 was minimized.

with any geographic parameter such as altitude. Using only potential terms involving sources internal to the region of measurement, it was impossible to obtain a fit whose average residuals did not systematically vary with altitude. Thus, for interpretation of temporal disturbances of the field, the computed residuals from the ΔF^2 fit were referred to the empirical curve drawn over the right most graph of Figure 2. That is, instead of considering the quantities ΔF for study the following slight modification was used:

$$\Delta F' = \Delta F + 0.011 (h - 1700), \quad (4)$$

for $h > 1700$ Km with no alterations below 1700 Km. This simple straight line modification was chosen as the most accurate warranted by the indicated standard error bars.

Before attempting to interpret Figure 2, it is useful to consider the overall residuals and estimates of the experimental errors of measurement. Plotted in Figure 3 are the distributions of absolute (ΔF) and relative ($\Delta F/F$) residuals from the set of 63 spherical harmonics used in the center graph of Figure 2. The 21 γ residual to the data indicated here is a marked improvement over the 255 γ residual found when the data were compared with the field computed from the Finch and Leaton [1957] coefficients. As seen in this figure, the residuals generally follow a Gaussian distribution except for a pronounced negative tail. The use of a larger number of harmonic coefficients was not useful for appreciably reducing the RMS residual.

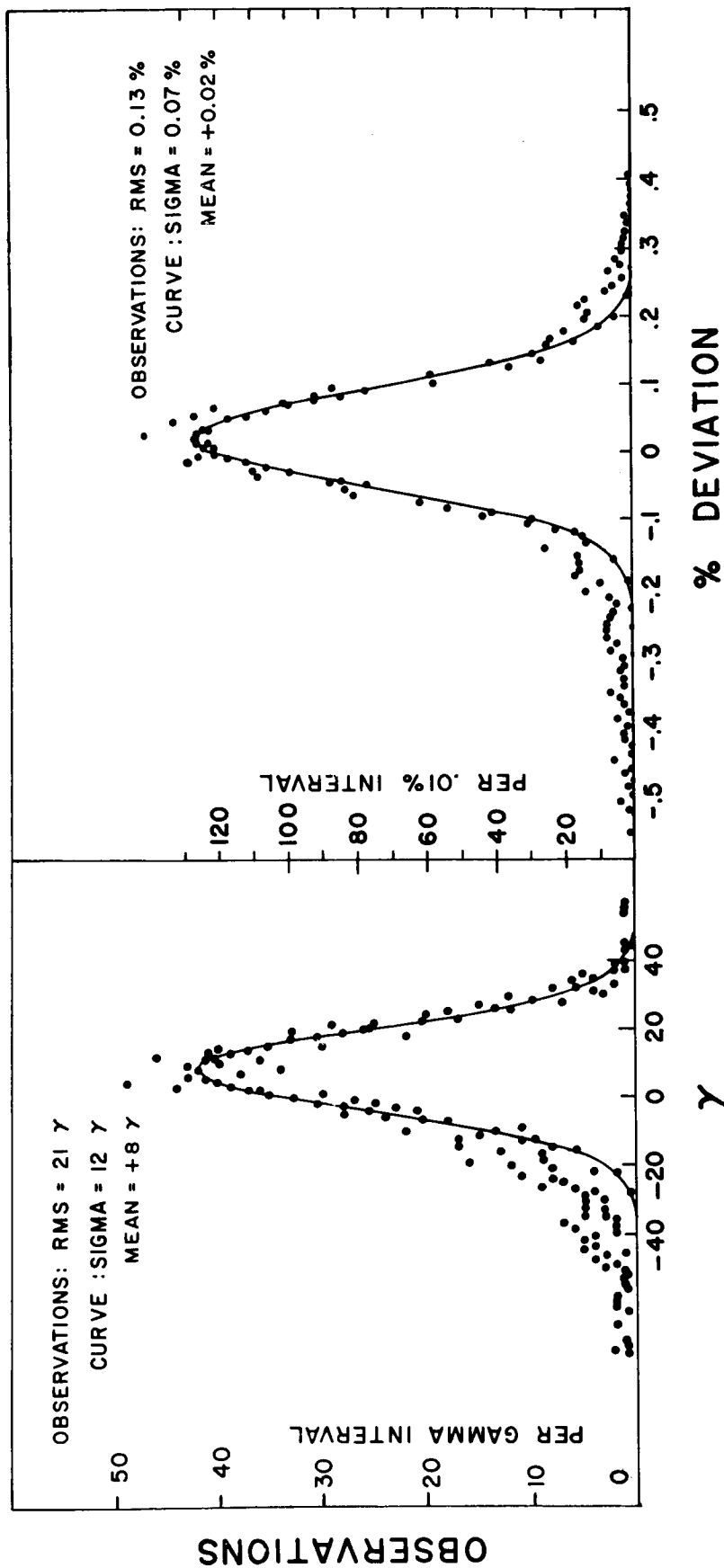


Figure 3-Distribution of measured values from those computed using a set of 63 spherical harmonics fitted to the data. Shown are both the absolute residuals (left) and relative residuals (right) including Gaussian curves to fit the central data.

Sources of Error

One may consider the sources of error that might randomly affect the data and thus give rise to the Gaussian part of these curves. Such errors would constitute a statistical "noise level" above which the time fluctuations would need to rise in order to be identifiable as real physical effects. The known sources of error are as follows:

- (1) Residual magnetism in the instrument package -- on the basis of preflight tests it is believed that this source of error was, at most, one gamma.
- (2) Vehicle rotation -- after about the second day from launch the satellite was rotating about an axis perpendicular to the original spin axis (same as coil axis) with a period of approximately 12 seconds. The contribution of the rotation frequency, 0.09 cps, to the measured frequency produces a 2γ average error following the formulation by Bloom [1955] illustrated by Heppner, Stolarik, and Meredith [1958a].
- (3) Signal noise -- the presence of noise in the demodulated magnetometer signal was estimated by the differences in the reduced magnetic field as determined by two or more recordings of the same magnetometer transmission at separate receivers. The statistics of the differences implied an RMS error of the order of 3γ .
- (4) Errors in coded time -- although large errors (hour, minute, or tens of seconds digits) in the recorded time were sometimes detected and the measurements either deleted or the time digit corrected, no contribution to the overall error caused by unnoted

time errors is indicated. These would have to occur in the seconds (as less than several seconds error) or tenths of second digits to have an unnoticed effect.

(5) Errors in computation of a reference field resulting from errors in estimating the position of the satellite at the times of magnetic field measurements -- this is the most significant source of error in the computation of ΔF and one of the most difficult to estimate. A total of nine different orbits for the active life of this satellite was computed by the Data Systems Division of the Goddard Space Flight Center (GSFC) and by the Smithsonian Astrophysical Observatory (SAO) during the two years since satellite launch. Since there is no fundamental way to verify the accuracy of a satellite orbit, checking could only be done by cross comparing the positions computed by these various orbits. Positions were determined at five minute intervals over the active life of the satellite and the magnetic field computed (using Finch and Leaton coefficients) at each position. Both the differences in position (longitude, latitude and altitude) and in computed total field were compared. That is, if the positions given by G (degrees longitude), T (degrees latitude), A (kilometers altitude), and B (gammas total field) are determined from orbits i and j, then the quantities investigated were:

$$\Delta G = G_i - G_j$$

$$\Delta T = T_i - T_j$$

$$\Delta A = A_i - A_j$$

and

$$\Delta B = B_i - B_j$$

This last quantity, of course, is directly related to the calculations of ΔF . These quantities were computed for several combinations of the nine orbits and the RMS, mean, and maximum values tabulated for each of the 85 days. None of the nine orbits was completely free of periods of one or more days when the computed positions disagreed grossly from those computed using several of the other orbits. The two best orbits (denoted here GSFC and SAO according to their origins) are compared in Table 1.

Table 1

Orbit Comparison

	RMS	Mean (GSFC-SAO)	Maximum
ΔT = Latitude (degrees)	.025	+.001	.058
ΔG = Longitude (degrees)	.023	-.016	.080
ΔA = Altitude (Km)	1.13	+.18	3.96
ΔR = Separation (Km)	5.1	-	11.5
ΔB = Field (gamma)	9	-7	51

Shown in this table are the Root-Mean-Square (RMS), mean (GSFC-SAO), and absolute maximum differences comparing in 5-minute intervals over the whole 85 day period. Additional details of this comparison are given elsewhere [Cain, Stolarik, Shapiro, and Heppner,

1962]. Similar comparisons made at intervals of one minute or even at times of the magnetic field observations give essentially the same results.

Assuming that the above errors are random and uncorrelated, one can obtain an overall estimate for the experiment. Summarizing, they are then:

1) Residual magnetism in package	1 gamma
2) Satellite rotation	2 gamma
3) Signal noise	3 gamma
4) Orbital error	9 gamma

for an estimated total error of $\sqrt{1^2 + 2^2 + 3^2 + 9^2} = 10\gamma$. Figure 3 illustrates that the distribution of differences from the fitted field consists of a Gaussian core having a 10γ dispersion plus a large negative and smaller positive tail. A study of the orbital differences suggests that a small part of this non-Gaussian component could arise from orbital errors. However, we postulate here that the major portion of this component is the result of magnetic disturbance whose main effect is to reduce the total field and thus produce the larger negative tail. It is then assumed that the statistical noise level of the data is of the order of 12γ and that most of the remaining dispersion is due to real field fluctuations.

4. Results

Altitude Variation

The systematic curvature of the residual plots in Figure 2 could be interpreted as implying sources in or above this region of

measurement which would produce the more negative residuals at higher altitude. It would not be difficult to concoct reasonable distributions of trapped particles that would match these curves. However, it is also possible that this effect could be caused by the way the data are distributed with local time and altitude. The distribution of the data is indicated in Table 2. As seen in this table, the perigee observations were predominantly taken during darkness whereas the high altitude data were mainly during the daylight hours. It is well known that at the earth's surface, even during magnetically quiet conditions, there is a daytime increase of total field intensity within $\pm 25^\circ$ of the geomagnetic equator with more complex fluctuations at higher latitude [Vestine et al., 1947]. In addition, there is an enhancement of this diurnal variation to an amplitude of approximately 100γ within a few degrees of the geomagnetic equator [Chapman, 1951, Onwumechilli, 1959, Forbush and Casaverde, 1961]. Generally, under magnetically quiet conditions, this field increase is observed only between 5^h and 18^h local time with a peak at about 11^h . Table 2 shows that the only equatorial data for which any altitude vs. local time effects might be separated lie between about 1500 and 3300 Km. The data for this altitude range have been studied in detail for various latitude ranges and selections of magnetic activity without finding any diurnal effect. This result is, however, inconclusive. If the data are selected by latitude to include only magnetically quiet intervals, there are not enough observations in a given grouping to discern any but large effects from the 12γ noise level. If the Sq variations do arise from ionospheric currents and if the earth is highly

Table 2

Distribution of Vanguard III magnetic observations by altitude and local time. The numbers under a local time t indicate the number of data for each altitude range in the local time interval $t - 1^h \leq t < t + 1^h$.

Altitude (Km)	Local Time (Hours)												Σ Day
	0	2	4	6	8	10	12	14	16	18	20	22	
500-700	75	170	188	19									452
700-900	70	30	34	43								13	190
900-1100	76		18	40	30							32	196
1100-1300	38		18	38	66						11	75	246
1300-1500	12			35	58	1					14	71	191
1500-1700				18	53	8				3	31	41	154
1700-1900				12	52	35				14	37	36	186
1900-2100				2	37	47				12	42	8	148
2100-2300					31	51				26	45	3	156
2300-2500					23	38	4			28	25		118
2500-2700					4	39	35		6	35	13		132
2700-2900					1	42	38	-	9	33	7		130
2900-3100						13	36	1	17	38	6		111
3100-3300						20	24	8	21	26			99
3300-3500						4	32	23	21	10			90
3500-3700							25	61	26	16			128
3700-3900							10	38	22				70
	Total Data												2797

conducting at depths not more than a few hundred kilometers below the surface, simple calculations, similar to those by Chapman [1951], show that the maximum Sq amplitude above 1000 Km would be no more than ten or twenty gamma. The diurnal variations could thus be detected only by data well distributed in local time and below 1000 Km altitude.

Storm-Time Effects

Before discussing the correlation between the satellite and surface observations, it is useful to summarize the behavior of the latter during the interval of measurement. Because of the previously mentioned local-time vs. altitude distribution of the satellite observations, this correlation is first considered by eliminating local time effects. Figures 4 and 5 give, respectively, the average daily intensities of the horizontal and vertical components of the magnetic field for a selection of standard observatories (see Figure 1). As is well known, there is a high correlation in disturbance of the horizontal component over a wide range of latitudes. Except for the high latitude station Sitka (+60° geomagnetic latitude) the amplitudes of the changes are essentially the same. As seen in Figure 5, the correlation in the vertical component between observatories is less noticeable with most stations showing very little average change from day to day.

The bottom curve of Figure 6 is the deviation ΔH from an average of the curves in Figure 4 for four low latitude observatories (Honolulu, Guam, Vassouras, and Huancayo). The top curve is the average daily residual $\Delta F'$ (modified ΔF as defined by Equation 4). The correlation between these two curves is striking. In an effort to consider the way

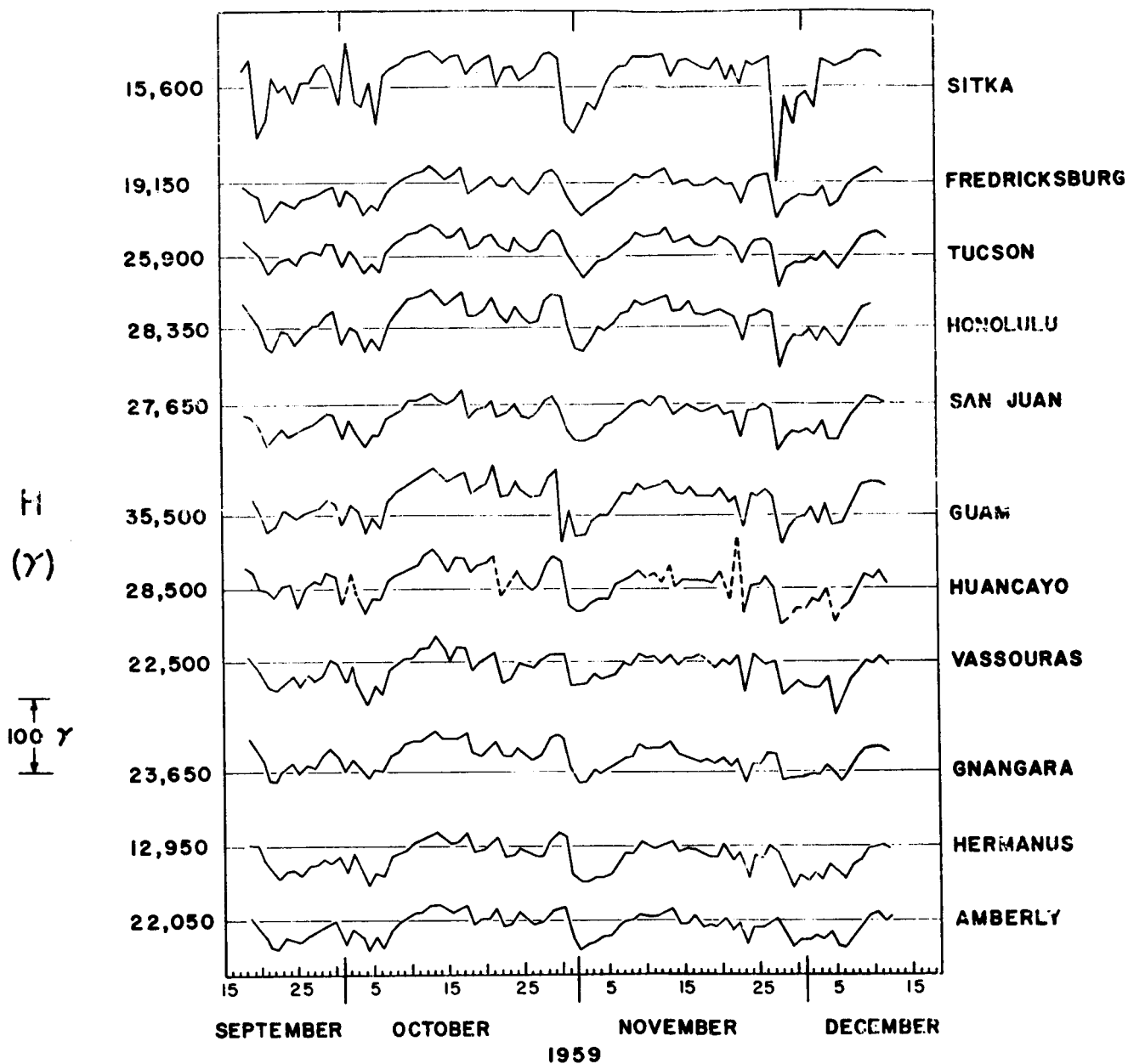


Figure 4—Average daily horizontal intensity of the geomagnetic field as measured at eleven observatories. Dashed lines are indicative that part of the day's data is missing and that the curve is there based on the available portion.

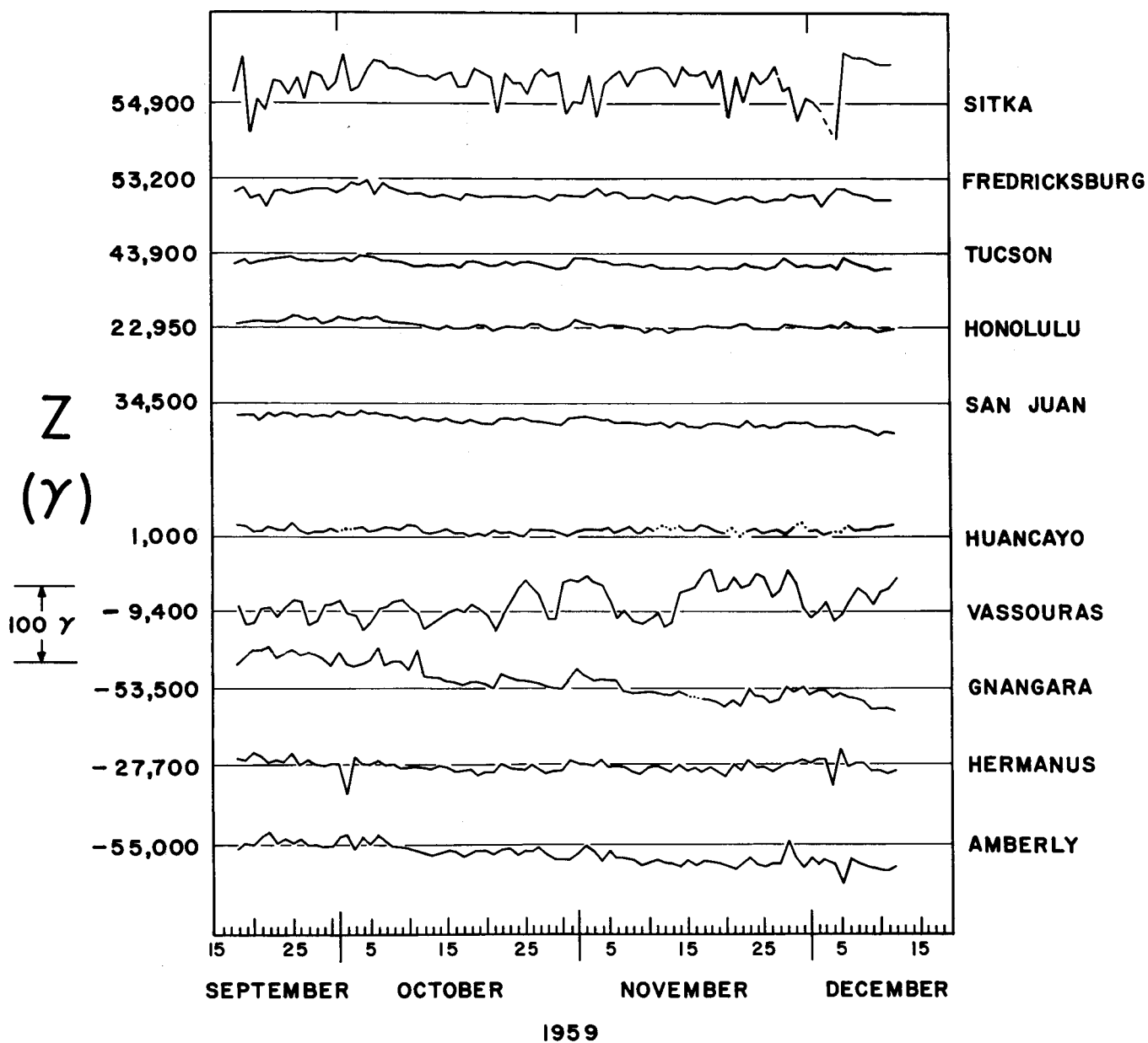


Figure 5—Average daily vertical intensities of the geomagnetic field corresponding to the same observatories as in 4 except Guam.

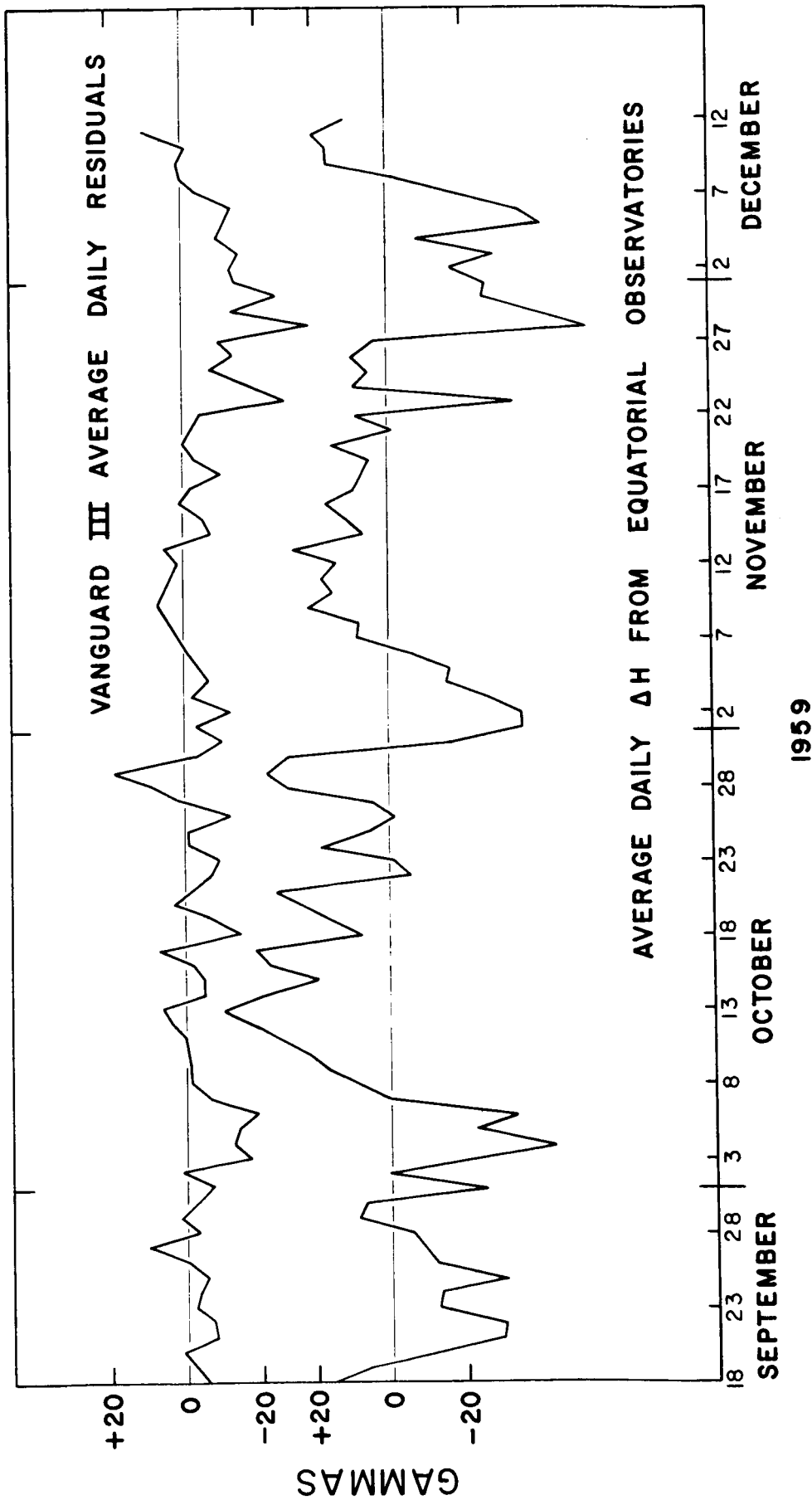


Figure 6-Vanguard III average daily residuals ΔF and average daily horizontal intensity ΔH from equatorial observatories. Both curves are plotted as differences from the 85 day mean Sept. 18 - Dec. 11, 1959.

in which these daily average fluctuations in total field might vary with latitude, a simple ring-current model is considered in Figure 7. Here is drawn for a dipole field the contribution to the total scalar field of a small disturbance vector directed towards the geomagnetic equator. This type of disturbance field is approximately that expected from a flux of particles trapped in the geomagnetic field [Akasofu, Cain and Chapman, 1961, 1962]. On the basis of this model, one would expect the change of the scalar field to be $\Delta B \cong D \cos \chi$ where D is the magnitude of the disturbance vector and χ is the angle between \underline{D} and the geomagnetic field \underline{B} . For a dipole field the value of $\cos \chi$ is given by

$$\frac{-1 + 3 \sin^2 \lambda}{\sqrt{1 + 3 \sin^2 \lambda}}$$

where λ = the geomagnetic latitude. This function is -1 at $\lambda = 0$, becomes zero at $\lambda = 35.2^\circ$ and is positive thereafter. On this basis, it would seem that such a disturbance field would decrease B below 35.2° and increase it above this latitude. To partially take into account the real geomagnetic field rather than the dipole field, the data are considered as a function of dip angle. The relation between the dip angle ϕ and the geomagnetic latitude λ for a dipole field is $\tan \phi = 2 \tan \lambda$. Thus $\cos \chi$ would pass through zero for $\phi = \tan^{-1} \sqrt{2} = 55.4^\circ$. Figure 8 is a histogram of the distribution of Vanguard III magnetic data with dip angle computed from a field calculated with the Finch and Leaton [1957] set of spherical harmonic coefficients using the known geographic positions of the observations. The values of $\cos \chi$ and equivalent geomagnetic latitude λ based on their values as computed from the above dipole field relations are added to the diagram.

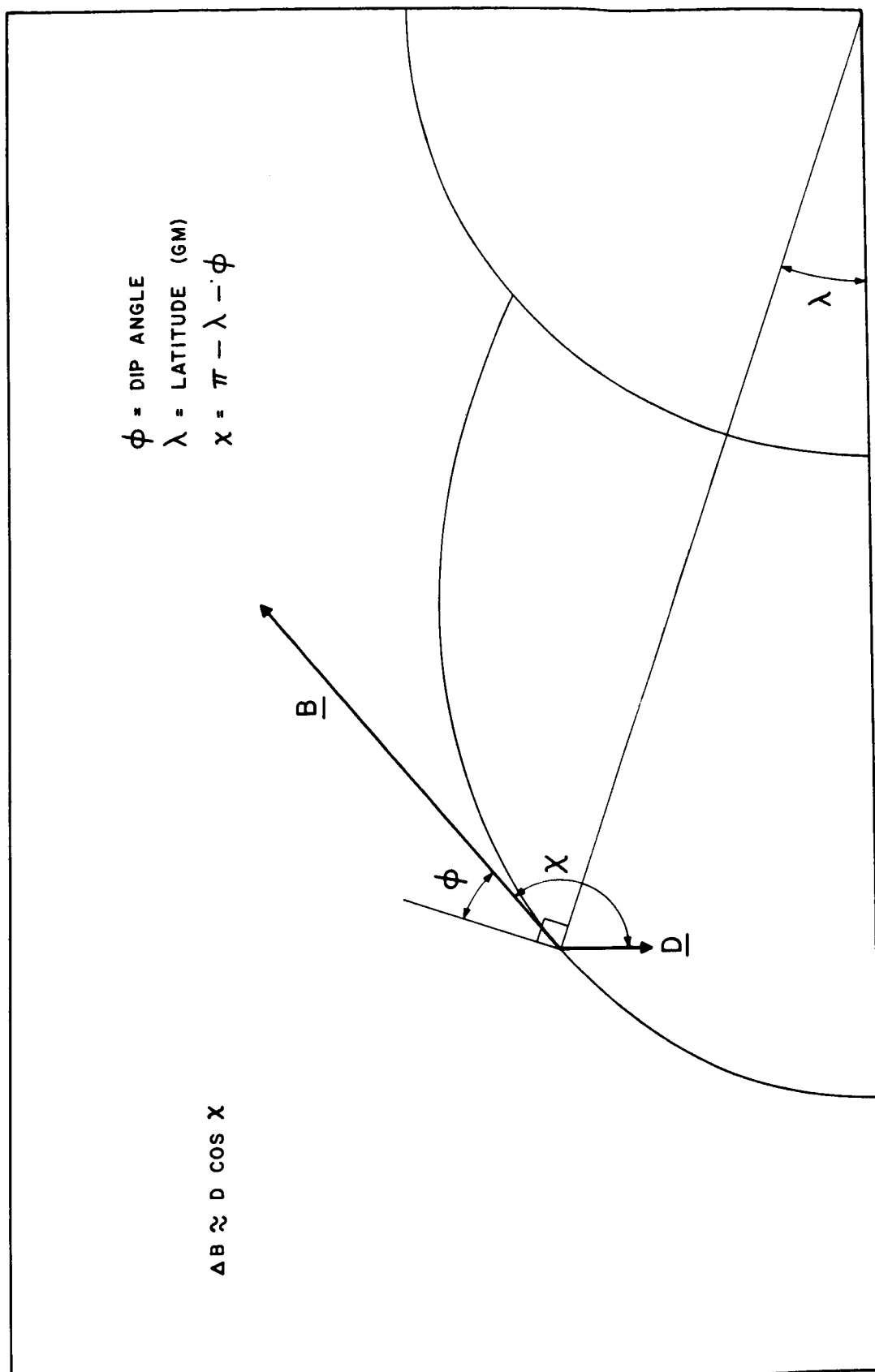


Figure 7—Contribution to the total scalar field B of a small disturbance vector directed towards the geomagnetic (dipole) equator.

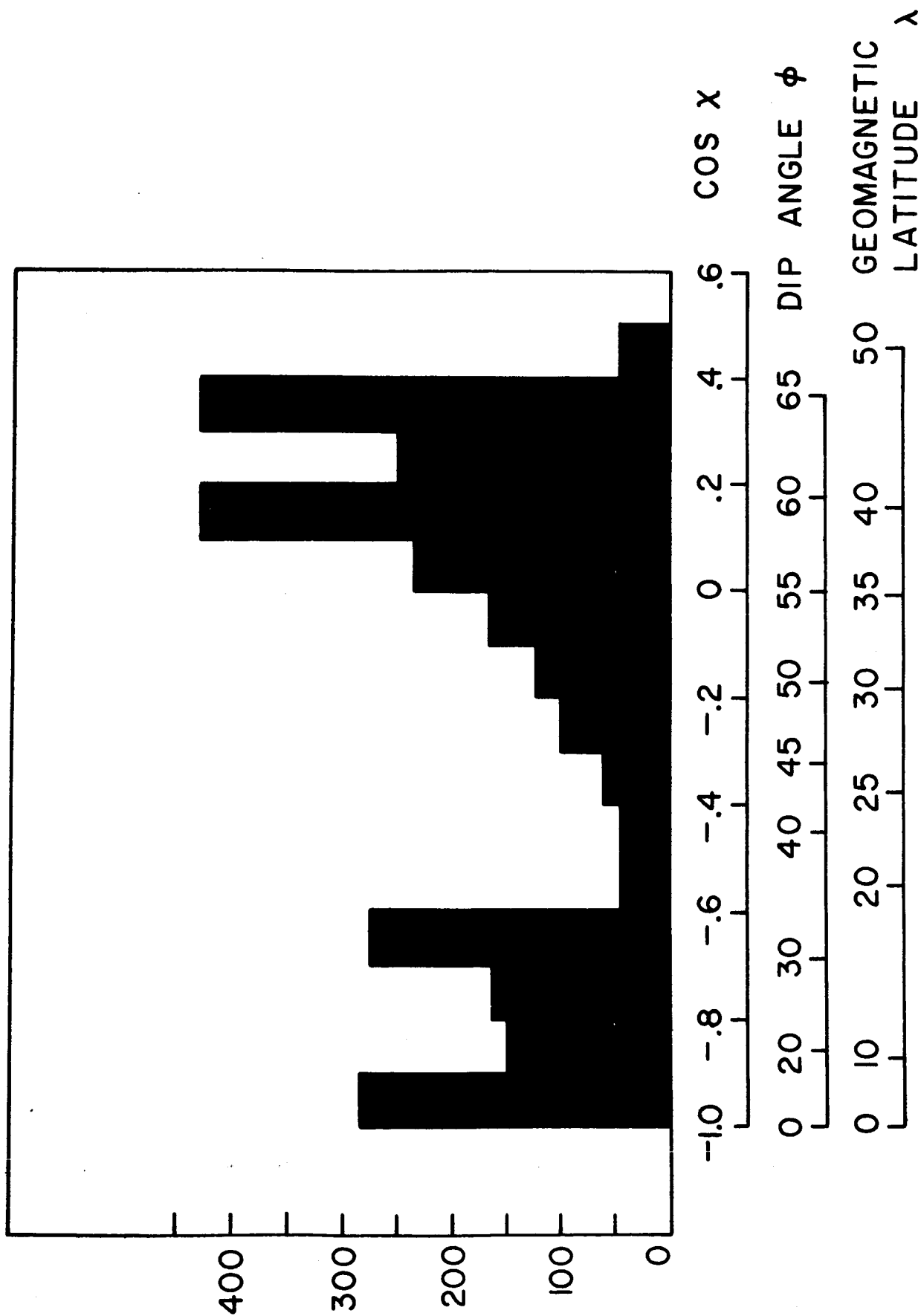


Figure 8--Distribution of Vanguard III magnetic field observations. The dip angle was computed from the position using the Finch and Leaton coefficients. $\cos \chi$ and the geomagnetic latitude λ were computed using dipole relations (see text).

Figure 9 gives scatter diagrams for the average daily modified residual $\Delta F'$ versus the average daily equatorial field ΔH (lower curve in Figure 6). The division of data for computing the average ΔF is based on a dip angle calculated using the Finch and Leaton [1957] set of coefficients. In the lower right of each of the three graphs is shown the linear correlation coefficient between the daily average ΔH and corresponding $\Delta F'$. On the basis of the simple model illustrated in Figure 7, the correlations should have been positive, near zero, and negative respectively in the three graphs of Figure 9. One possible complicating factor which could make all three correlations positive has to do with the effect of induced currents in the earth and also possibly in the ionosphere. As has been shown by Price [1930, 1932] the effect of induced earth currents on the periodic variations of the field at the surface enhances the amplitude of the changes in the horizontal component and reduces those in the vertical. The lack of correlation of the changes in the daily average vertical component with fluctuations in the horizontal component is clearly evidenced by comparing the various curves on Figure 5 with those for the same observatory on Figure 4. Only by using more refined analysis techniques is it possible to determine the weak ($<10\gamma$) response of the vertical component to average magnetic disturbance [Sugiura and Chapman, 1960]. Without a detailed knowledge of the conductivity of the earth it is not possible to predict the way in which the induced currents would affect an external source field. The relative correlations in Figure 9 cannot be computed by simple distortions of an axial disturbance field. The high

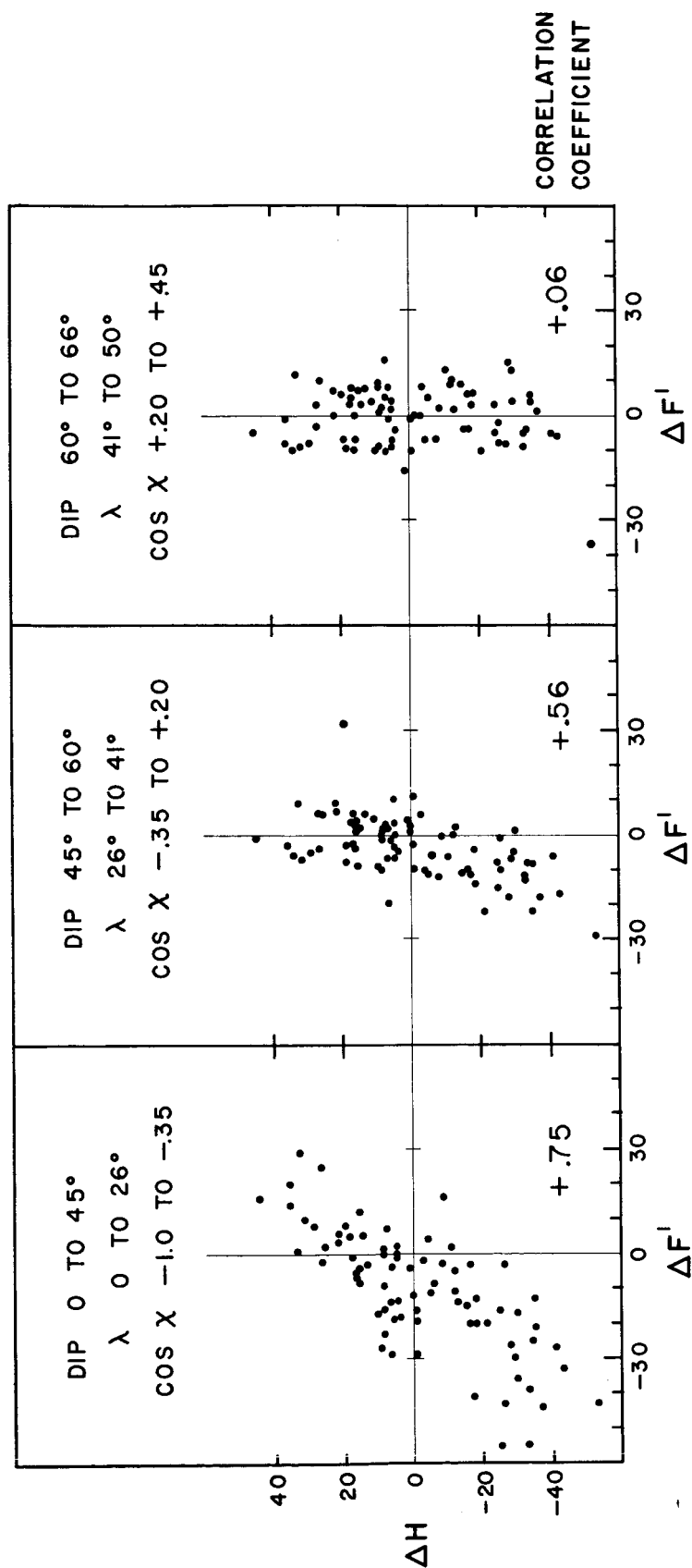


Figure 9—Scatter diagrams giving the correlation between the average daily equatorial horizontal intensity ΔH and the average daily residual $\Delta F'$. Data are selected by dip angle as computed by the Finch and Leaton coefficients. Geomagnetic latitude and $\cos \lambda$ (see text) are derived from the dip using dipole relations. Linear correlation coefficients are indicated in lower right of each figure.

correlation in the middle diagram could result from a disturbance field that is essentially horizontal. However, the small positive correlation for the higher latitude data ($60 < \phi < 66^\circ$) would imply a disturbance field approximately perpendicular to the main field and having a dip angle of 20 to 25°S. Regardless of the exact geometry of this disturbance vector, Figure 9 clearly shows that the source of these changes is predominantly above the 510-3753 Km region of measurement. Further divisions of the data by altitude have been made and do not negate this conclusion even for data above 2400 Km. However, the fluctuations of the average daily residuals become larger when the data are further subdivided according to location as a consequence of not having random time sampling. Thus the correlation becomes poorer even for low latitude data and an accurate comparison over smaller altitude intervals is not possible using daily averages.

Having established the high correlation between the daily average surface and satellite magnetic field observations, it is useful to consider next whether there are any systematic changes when the individual satellite observations are compared with those taken in the same area at the surface. Due to the estimated 12 γ RMS error of the satellite data, it is dangerous to draw conclusions from a single datum unless the fluctuations are several times this amount. Also, experience in reducing the satellite data has shown that it is possible to obtain spurious readings due to telemetry noise or incorrect time recording. The procedure followed in the data reduction was to delete any observations with a high ΔF if the signal was noisy or if time errors were suspected.

Fortunately, duplicate recordings of the same signals by two or more stations made it possible to verify many of the data taken over South America. There were a few middle-latitude observations with ΔF of the order of ± 100 or $\pm 200 \gamma$ that could not be discounted by reason of suspected error. These few anomalous observations were not always correlated with magnetic disturbance and generally occurred on single data tapes from isolated stations ("Nelcal" and Blossom Point) where it was impossible to verify their values by duplicate recordings.

The sharp negative changes on Figure 4 are all in response to recognized magnetic disturbances. Generally, the periods of increasing H at all stations are during the recovery phases of these disturbances. Comparing Figure 4 with a listing of the reported magnetic disturbances [Lincoln, 1960, 1961] it is apparent that the smaller negative fluctuations are unreported at many observatories even though an average daily depression of H seemed to occur at almost all stations. A qualitative survey of the magnetic activity during the period of satellite measurement on the basis of the observatory reports is listed as follows:

A) Sept. 18-27: Several moderate to severe disturbances spaced irregularly throughout the interval reported at less than five observatories at once. Most of the activity began about 11^h 57^m Sept. 20 when a sc was reported at five observatories with the storm ending at 21^h on Sept. 22.

B) Sept. 27-Oct. 1: No reported disturbance.

C) Oct. 1-8: A series of moderate to moderately severe disturbances each of about a day's duration with only one weak sc reported by one station.

D) Oct. 8-17: No reported disturbance.

E) Oct. 17-19: A moderate disturbance reported at six observatories with no clear sc.

F) Oct. 19-29: Two short moderately severe disturbances reported at only two observatories.

G) Oct. 29-Nov. 7: A moderately severe disturbance beginning with an sc reported by 11 observatories at about 23^h48^m October 29. This disturbance continued at some stations through most of this interval or was followed by newly reported disturbances with no recognizable sc's.

H) Nov. 7-21: Quiet except for a short disturbance Nov. 14 reported at only three observatories.

I) Nov. 21-27: One or more short disturbances reported by five observatories and ending by Nov. 24.

J) Nov. 27-29: A short moderately severe to severe storm with an sc reported at 17 observatories about 23^h51^m on Nov. 27 and ending by 2^h on Nov. 29 at most stations.

K) Nov. 29-Dec. 5: Moderate to severe disturbances throughout most of the interval first reported on Nov. 30 and ending at almost all stations by Dec. 4.

L) Dec. 5-Dec. 11: A moderately severe to severe storm with an sc reported at 16 observatories at about 6^h59^m Dec. 5 and ending at

almost all stations on Dec. 6. No disturbance reported after Dec. 7.

The detailed correlation between the satellite measurements and the storm-time fluctuations was investigated for the intervals indicated above by A), C), G), I), J) and L). Generally, this study merely confirmed the conclusions already reached by investigating the average daily correlations. The problem of correlating in detail is of course increased by the discontinuous nature of the satellite observations both in space and time. Samples of this correlation are indicated in Figures 10 and 11 for the storms occurring in intervals I) and L) respectively. The top curves for each of these figures are approximate Dst curves for two equatorial observatories obtained by subtracting an average Sq from each. The satellite observations plotted on the lower curves are the modified residuals $\Delta F'$ using different symbols for different computed dip angles (as in Figure 9). Although these data are somewhat sparse, those for the lower latitudes ($0 < \phi(\text{inclination}) < 45^\circ$) show a remarkable resemblance to the Dst curves.

5. Conclusions

The Vanguard III magnetic experiment has demonstrated that it is possible to measure only total scalar field and derive some meaningful information concerning field fluctuations in equatorial regions. There is now no question that the primary source of the Dst magnetic storm variation lies above 500 Km and it is very likely that it lies above 2400 Km altitude. Within the range of measurement the behavior of

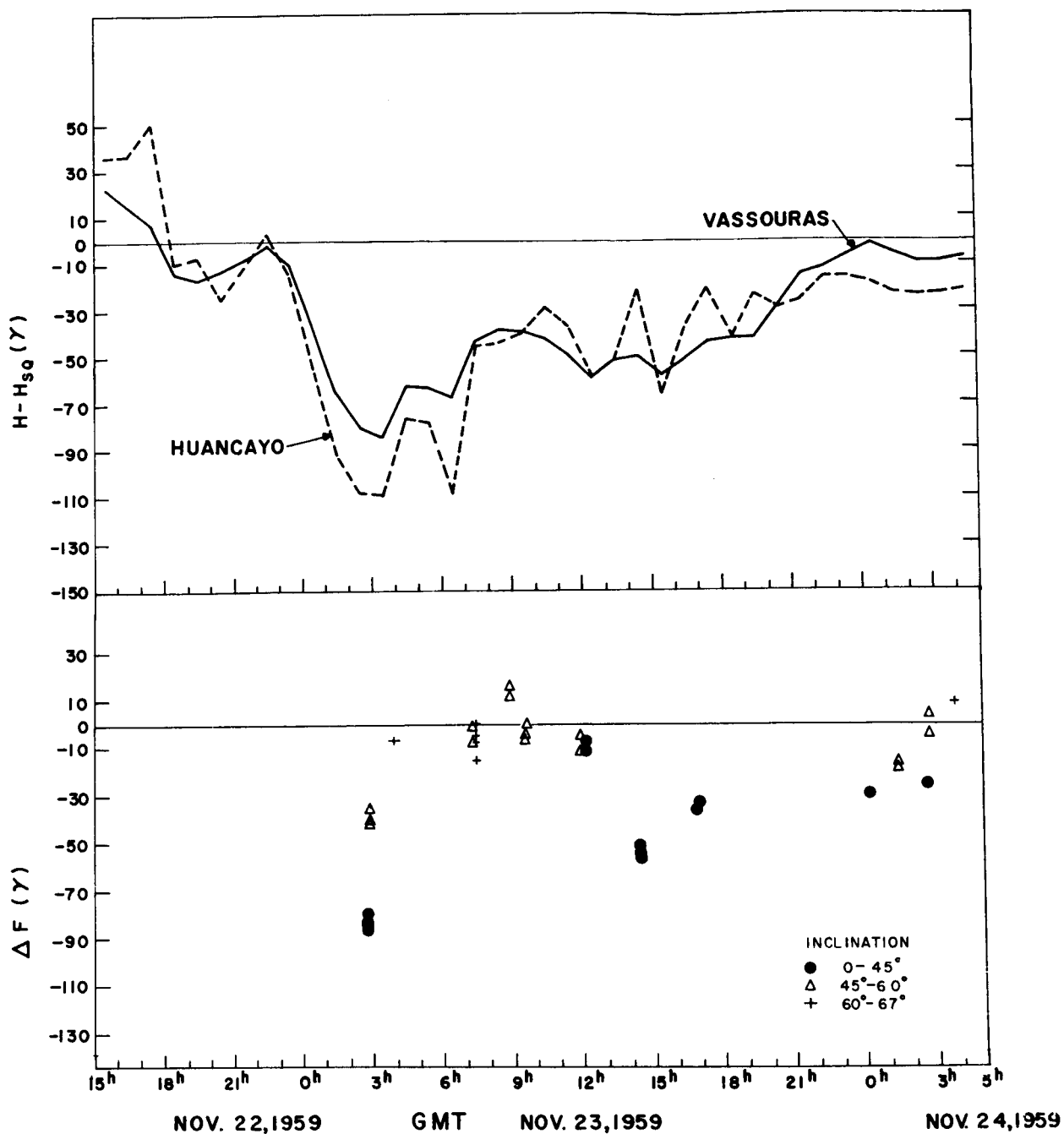


Figure 10—Hourly average disturbance ($H - H(Sq)$) in the horizontal field at two equatorial observatories (top graph). Modified residuals $\Delta F'$ for individual satellite observations (bottom graph). Inclination assigned according to field computation using Finch and Leaton coefficients.

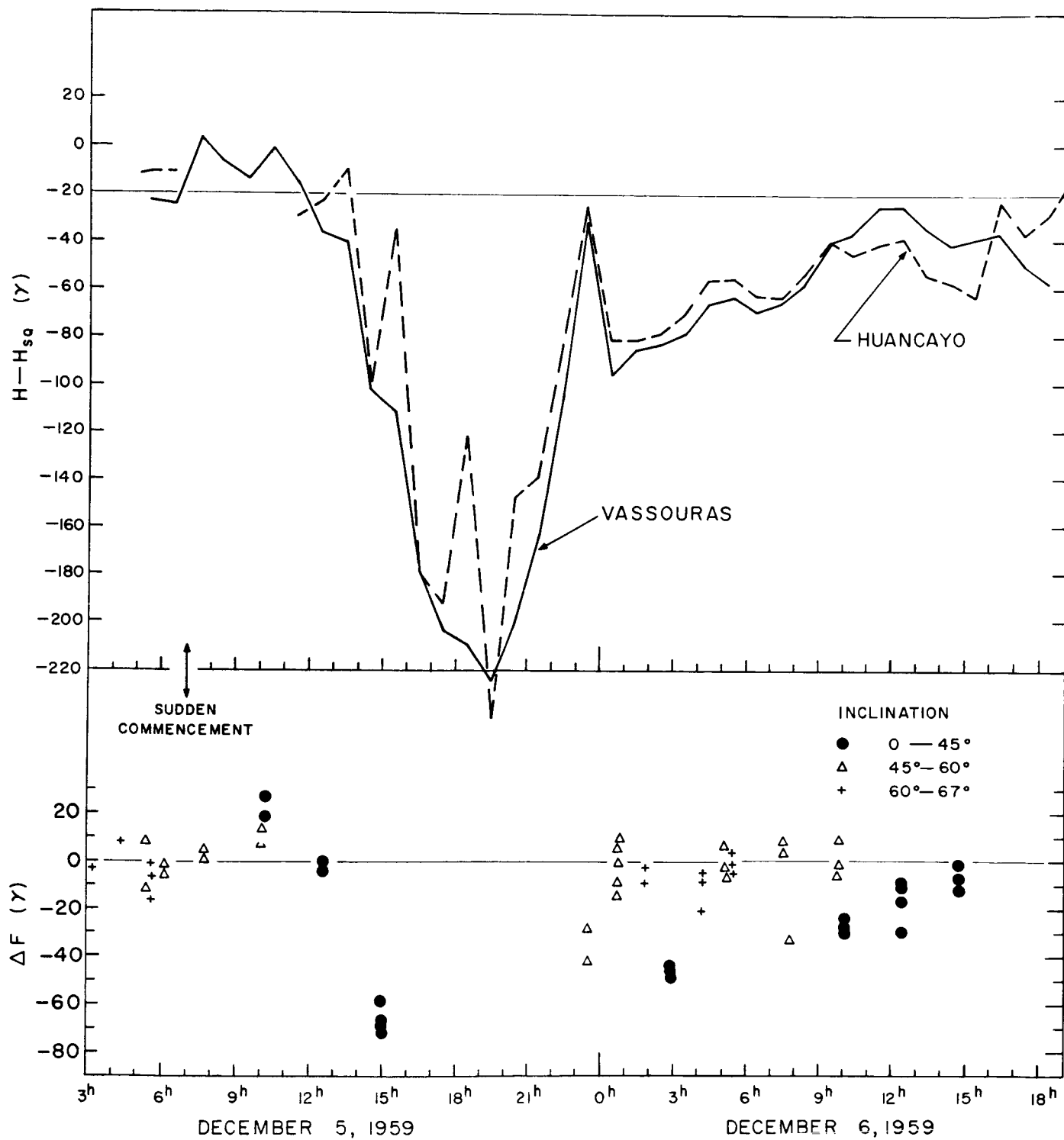


Figure 11—See Figure 10.

Dst (F) at low latitudes is substantially the same as that observed at the earth's surface.

It was demonstrated that it is possible to compute the scalar field to within an RMS error of the order of 20γ or about 0.1% using spherical harmonic terms of internal sources. A smaller systematic variation of the field with altitude was noted that appeared to require external sources, but the distribution of data with local time and altitude was insufficient to conclude that the effect was not diurnal. For this reason also no conclusions could be drawn concerning the location of the sources of the DS or SD and Sq magnetic variations including the equatorial electrojet.

Acknowledgment

This is to acknowledge the assistance of the Smithsonian Astrophysical Observatory in providing orbital programs and several sets of elements especially computed for our analysis. We would also like to acknowledge several helpful suggestions by N. F. Ness and E. C. Ray during the analysis and by M. Sugiura during preparation of the manuscript. Important contributions were also made by S. Hendricks and W. E. Daniels in the course of the data reduction and analysis.

References

- Akasofu, S-I, J. C. Cain and S. Chapman, The magnetic field of a model radiation belt, numerically computed, J. Geophys. Res., 66, 4013-4026, 1961.
- Akasofu, S-I, J. C. Cain and S. Chapman, The magnetic field of the quiet-time proton belt, J. Geophys. Res., 67, (July) 1962.
- Alexander, W. M., C. W. McCracken and H. E. LaGow, Interplanetary dust particles of micron-size probably associated with the Leonid meteor stream, J. Geophys. Res., 66, 3970-3973, 1961.
- Bloom, A. L., Nuclear-free precession in a moving vehicle, Technical Memorandum, Varian Associates, 1955.
- Cahill, L. J., Investigation of the equatorial electrojet by rocket magnetometer, J. Geophys. Res., 64, 489-503, 1959a.
- Cahill, L. J., Magnetic exploration of the upper atmosphere, IGY Rocket Report Series, No. 4, Oct., 1959b.
- Cain, J. C., J. D. Stolarik, I. R. Shapiro, J. P. Heppner, Measurements of the geomagnetic field by the Vanguard III satellite, NASA TND-1418, 1962.
- Chapman, S., The equatorial electrojet as detected from the abnormal electric current distribution above Huancayo, Peru, and elsewhere, Arch. Meteorol. Geophys. u, Bioklimatol, 4, 1951.

Chapman, S. and J. Bartels, Geomagnetism, Oxford University Press, London, 1940.

Finch, H. F. and B. R. Leaton, The earth's main magnetic field -- Epoch 1955.0, Monthly Not. Roy. Astron. Soc., Geophys. Supplement 7 (6), 314-317, November, 1957.

Forbush, S. E. and M. Casaverde, Equatorial electrojet in Peru, Carnegie Institution of Washington Publication 620, 1961.

Heppner, J. P., T. L. Skillman and J. C. Cain, Contributions of rockets and satellites to the world magnetic survey, Space Research II, Proceedings of Second International Space Science Symposium, Florence, 681-691, 1961.

Heppner, J. P., J. D. Stolarik and L. H. Meredith, The earth's magnetic field above WSPG, New Mexico, from rocket measurements, J. Geophys. Res. 63, 277-288, 1958a.

Heppner, J. P., J. D. Stolarik and L. H. Meredith, A review of instrumentation for magnetic-field satellite experiment, Annals of IGY, Vol. VI, 323-328, 1958b.

Jensen, D. C. and J. C. Cain, An interim geomagnetic field, (abstract), Meeting of American Geophysical Union, Washington, D. C., April 1962.

Jensen, D. C. and W. A. Whitaker, Spheric harmonic analysis of the geomagnetic field, Meeting of American Geophysical Union, Washington, D. C., April, 1960.

Lincoln, J. Virginia, Geomagnetic and solar data, J. Geophys. Res.,
65, 795-797, 1323-1326, 1960.

Lincoln, J. Virginia, Geomagnetic and solar data, J. Geophys. Res.,
66, 314, 662, 1282, 1961.

Onwumechilli, C. A., A study of the equatorial electrojet -- I, II, Journal
of Atmospheric & Terrestrial Physics, 13, 222-257, 1959.

Price, A. T., Electromagnetic induction in a sphere, Proc. London
Math. Soc. 31, 217-224, 1930.

Price, A. T., Electromagnetic induction in a sphere, Proc. London
Math. Soc. 33, 233-245, 1932.

Shapiro, I. R., J. D. Stolarik and J. P. Heppner, The vector field proton
magnetometer for IGY satellite ground stations, J. Geophys. Res. 65,
913-920, 1960.

Singer, S. F., E. Maple, and W. A. Bowen, Evidence for ionosphere
currents from rocket experiments near the geomagnetic equator,
J. Geophys. Res. 56, 265-281, 1951.

Sugiura, M. and S. Chapman, The average morphology of geomagnetic
storms with sudden commencement, Abhandl. Akad. Wiss. Göttingen,
Math-Phys. Klasse., Sonderheft Nr. 4, 1960.

Vestine, E. H., I. Lange, L. Laporte and W. E. Scott, The geomagnetic field, its description and analysis, Carnegie Institution of Washington Publication 580, 1947.

Zadunaisky, P. E. and B. Miller, Elements of the orbit of the satellite 1959 ETA (Vanguard III) during the first year after launching, SAO Special Report No. 71, 1961.